JPhys Energy

PAPER • OPEN ACCESS

Ultrathin Cu(In,Ga)Se_2 solar cells: enhanced absorption by nanotextured functional back contacts

To cite this article: M Demir *et al* 2025 *J. Phys. Energy* **7** 045003

Journal of Physics: Energy

PAPER

Ultrathin Cu(In,Ga)Se_2 solar cells: enhanced absorption by nanotextured functional back contacts

M Demir[1,*], D Jiménez Tejero[1], B Fuhrmann[2], H Kempa[1], A Sprafke[2] and R Scheer[1]

[1] Martin-Luther-University Halle-Wittenberg, Institute of Physics, Von-Danckelmann-Platz 3, 06120 Halle, Germany
[2] Interdisiplinary Center of Material Research, Heinrich-Damerow-Straße 4, Halle 06120, Germany
* Author to whom any correspondence should be addressed.

E-mail: merve.demir@physik.uni-halle.de

Keywords: ultrathin, solar, cells, enhanced, absorption, light management

Supplementary material for this article is available online

OPEN ACCESS

RECEIVED
28 February 2025

REVISED
1 June 2025

ACCEPTED FOR PUBLICATION
25 June 2025

PUBLISHED
15 July 2025

Abstract

Ultrathin Cu(In,Ga)Se_2 solar cell conversion efficiencies are limited by incomplete absorption of the solar spectrum. In this study, we experimentally investigate a light management strategy to enhance the performance of ultrathin Cu(In,Ga)Se_2 (CIGSe) solar cells through the implementation of a functional back contact with SiO_2 nanostructure scatterers and a planar gold reflector. External quantum efficiency (EQE) and current–voltage measurements reveal significant improvements in short-circuit current density (J_{sc}), with a notable increase from 21.6 mA cm^{-2} to 27 mA cm^{-2} with a 25% increase for 300 nm CIGSe absorbers when transitioning from conventional molybdenum back contacts to functional back contacts with 500 nm SiO_2 scatterers. This enhancement is attributed to a light trapping effect. Also, backside nanostructures imprint a height profile into all layers on top, which provides strongly suppressed front reflection. However, these gains are partially offset by reductions in open-circuit voltage (V_{oc}) and fill factor (FF) possibly due to shunt pathways introduced by the nanotextured architecture. The highest power conversion efficiency of 12.9% was achieved with a 500 nm CIGSe absorber and 500 nm SiO_2 scatterers, representing a 1.8% absolute efficiency gain over the reference Mo-based design. Optical simulations corroborate the experimental EQE trends, highlighting the role of nanostructure geometry in optimizing light absorption. Our findings demonstrate that carefully engineered light management structures can mitigate absorption losses in ultrathin CIGSe solar cells, providing the way for high-efficiency, cost-effective photovoltaic devices.

1. Introduction

Reducing the thickness of the standard Cu(In,Ga)Se_2 (CIGSe) solar cell absorber from 2–3 μm to a few hundred nanometers reduces material consumption and enables cost-effective large-scale production. However, ultra-thin CIGSe solar cells with absorber layer thicknesses at the sub-micron level limit the absorption of solar energy and increase losses due to enhanced back contact recombination [1, 2]. To date, the highest efficiency reported for an ultrathin CIGSe solar cell—with a 550 nm absorber layer on a flat molybdenum back contact—is 15.2%, achieved through the introduction of an effective back surface field via Ga grading and the realization of a high V_{oc} [3]. However, this cell suffered from poor quantum efficiency in the near infra-red (NIR) region of the spectrum. Oliveira *et al* showed that the open circuit voltage of ultrathin CIGSe solar cells is increased by rear passivation, achieving an efficiency of 13% for a 640 nm CIGSe solar cell featuring a SiO_x passivation layer [4]. Despite these successive attempts at resolving the recombination issue of ultrathin solar cells, efficiencies achieved by standard thick CIGSe solar cells, up to 23.6%, are still far off [5]. Therefore, in this work, we address another major issue of ultrathin CIGSe solar cells, i.e. incomplete light absorption.

Incomplete optical absorption of the ultrathin absorber can be overcome by a cell architecture including light management techniques [6, 7]. These can be macroscopic concepts, such as optimizing reflectivity by adjusting the thicknesses and the refractive index gradient of the front layers. For instance, the application of anti-reflection coatings is a well-known approach, for conventionally thick CIGSe solar cells [8]. Furthermore, nanoscopic light management techniques can be applied as functional back contacts or front texturing for the elongation of the light path within the cell and for the enhancement of absorption due to interference and resonant modes [9–12]. Increased roughness of periodic nano-structures can create enhanced electric field spots where the absorption is high due to multi-resonant standing waves. A comprehensive review on light management in chalcopyrite solar cells can be found in [13].

Different types of light management strategies have been suggested in the literature, either through optical simulations or by experimental findings, including nano meshes [14], metallic nanoparticles [15] or random front texturing [10]. However, as a review article on ultrathin solar cells shows [16], almost all experimental attempts with ultrathin CIGSe solar cells resulted in poorer device performance than the theoretical calculations suggest [16]. Therefore, we can conclude that even though the photonic effects in solar cells have been demonstrated, there is still no consensus on the discussion of the most favorable nanotexturing, cell design or the materials to be used for the absorption enhancement of ultrathin CIGSe solar cells.

Van Lare *et al* demonstrated SiO_2 nanoparticles on molybdenum back contact and observed an increase of 2 mA cm^{-2} in short circuit current density (J_{sc}) resulting in an efficiency of 12.3% for 460 nm CIGSe [17]. Later, Schneider *et al* combined SiO_2 nanotexturing with an aluminum metal reflector on top in order to harvest more light [18]. In our previous work, we reported the improvement in absorption when transitioning from a molybdenum back contact to a flat mirror, gold back contact. Moreover, we compared cell architectures where the metal reflector was placed either beneath or on top of nano elements. Additional resonant modes in the long wavelength region indicate that the metal reflector should be planar and positioned underneath the nano texturing elements [19].

Here, we propose a cell design with functional back contacts where SiO_2 pyramids periodically cover a gold metal reflector. The gold metal layer has been chosen due to its excellent reflectivity and, in particular, for its low chemical diffusivity. Furthermore, the thermal stability requirement concerning the high process temperatures of CIGSe layer, can be fulfilled by a In_2O_3:Sn (ITO) diffusion barrier. The experimental findings discussed in the following are aided by accompanying optical simulations.

2. Experimental details

Two different sets of solar cells were prepared with CIGSe absorber thicknesses of 300 and 500 nm. Commercial soda-lime glass covered with a sodium diffusion barrier and a molybdenum layer was used as the substrate. The back reflector metal, a 100 nm thick gold layer, was deposited by electron beam evaporation with initial 10 nm Cr adhesion layer, followed by 100 nm ITO as the metal diffusion barrier sputtered on top. Nano-textured SiO_2 layers were realized by laser interference lithography [20]. In this step, a deep UV negative photoresist (AR-N 4240, diluted with AR 300–12 1:0,75, Allresist) with an approximate thickness of 250 nm was applied by spin coating at 4000 rpm and exposed to a 266 nm laser beam through a Fresnel-type interferometer. After baking on a hotplate for 5 min at 95 °C and developing (AR 300–475, Allresist) of the photoresist for 45 s, a pretreatment in oxygen plasma for 3 min was performed. SiO_2 was deposited by e-beam evaporation to create the scattering elements. Back texturing was completed using a lift-off process in an ultrasonic bath with a remover solution (AR 300–76) for 30 min. Our optical simulations of nanotexturing parameters suggest a pitch value of 968 nm for the maximum achievable photocurrent (MAPC) for 500 nm absorber thickness. The experimental optimum pitch value achievable by our laser interference lithography setup is 1000 nm. We aimed to approximate the theoretical optimum pitch value as close as possible while investigating the effect of element height by varying it. Therefore, the resultant nano-texturing elements in a square lattice have a pitch of 1 μm and two different heights of 300 and 500 nm. An example of the nanotextured substrate is presented in figure 1(a).

CIGSe thin films were fabricated by physical vapor deposition in the so-called three-stage process [21]. The substrate temperature is set at 480 °C, relatively lower than standard CIGSe process temperatures (≈550 °C–600 °C). This adjustment ensures the chemical stability of the metal containing substrates and allows for better control of the Ga grating. The deposition took place under Se atmosphere where the first phase starts with the evaporation of In and Ga. The composition and thickness of the films were controlled by laser light scattering during the growth. In the second phase, Cu evaporated until the films reach Cu-rich phase. Deposition is completed by evaporation of In and Ga in the third stage which results in Cu-poor film

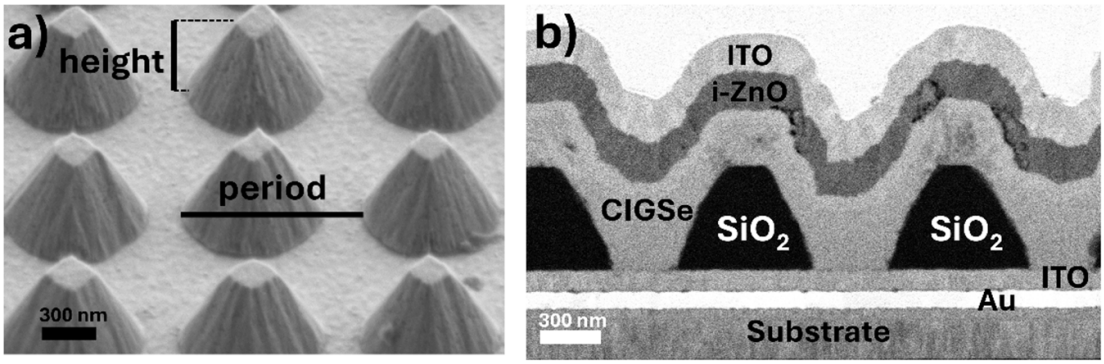

Figure 1. (a) Functional back contacts with SiO_2 nano structures, (b) scanning electron microscope (SEM) image of a focused ion beam (FIB) cross section of a solar cell; 300 nm CIGSe absorber on the functional back contact consists of flat Au reflector covered by 100 nm ITO diffusion barrier and 500 nm SiO_2 nanotexturing elements.

stoichiometry. Depth resolved GGI ([Ga]/([Ga] + [In])) and CGI ([Cu]/([Ga] + [In])) profiles were obtained using glow discharge optical emission spectroscopy (GDOES) and are presented in figure S1. Deposited CIGSe films show Ga gradient with an increment towards the back contact. Both films with different CIGSe thicknesses exhibited depth averaged GGI and CGI values of 0.37 and 0.79, respectively. All samples underwent NaF precursor and post deposition treatment. CIGSe thin films were completed to solar cells by coating 50 nm CdS by chemical bath deposition followed by 100 nm i-ZnO and 200 nm ITO front layers sputtering. Ni/Al/Ni metal grids were applied by e-beam evaporation. Solar cell separation was performed by chemical etching of TCO and CdS layers with HCl solution of 10% concentration using a fine brush.

I–V measurements were performed in a four-point configuration with a source meter under a class AAA solar simulator. External quantum efficiency (EQE) was measured with a dedicated home-built system in a four-point configuration as well. Optical simulations were performed using the specialized Maxwell solver software JCMsuite, based on the finite element method [22]. The refractive indices of Mo were obtained from [23] and those of Au from [24]. The optical data for the rest of the layers are the same as those used in [18]. The optical data for CdS and ZnO were taken from [25].

3. Results and discussion

Current densities derived from the EQE spectra are listed in table 1 together with open circuit voltages, FFs, and power conversion efficiencies of the solar cells. A V_{oc} of around 650 mV and a FF of 70% was reached for all reference solar cells on planar molybdenum back contact regardless of the CIGSe thickness. However, there is a decrease of J_{sc} as the absorber thickness goes down from 500 nm to 300 nm on Mo. This current loss is mitigated when functional back contacts are implemented. The highest relative gain in J_{sc} was observed in the case of 300 nm CIGSe absorber layer with an increase from 21.6 mA cm^{-2} on molybdenum to 27 mA cm^{-2} on a functional back contact. Conversely, slight reductions of V_{oc} and FF values were introduced by the functional back contacts. Lower V_{oc}, compared to standard thick solar cells, is a well-known issue of ultrathin CIGSe solar cells due to back contact recombination [1, 2]. This could explain the V_{oc} values of 650 mV for the presented solar cells on molybdenum. Yet, a further decrease in V_{oc} is observed upon implementing functional back contacts. This loss in V_{oc} could be attributed to enhanced interface recombination due to altered cell architecture as discussed below.

For ultrathin solar cells, the bulk recombination is not as severe as in their conventional thick designs due to the smaller volume of the absorber material [26]. Hence, recombination at the back interface can be a primary loss mechanism for ultrathin solar cells. As presented in the SEM cross section of figure 1(b), the functional back contact introduces a new interface namely the one between the dielectric SiO_2 nano elements and CIGSe. The rear surface area is increased by about 29% (with respect to the flat Mo back contact) due to the SiO_2 scattering elements. Similarly, the backside texturing increases the surface area of the CIGSe/CdS interface in comparison to the flat solar cell design. In general, an increased surface area leads to an increased number of recombination centers at the interfaces.

As shown in the current–voltage characteristics of the solar cells in figure S2, samples with functional back contacts exhibit higher shunt conductance in dark *J–V* measurements, except for an outlier 500 nm

Table 1. Solar cell parameters at simulated AM1.5 illumination of 300 and 500 nm CIGSe absorbers on different substrates as described in the text.

	Substrate	J_{sc} (mA cm^{-2})	V_{oc} (mV)	FF (%)	η (%)
300 nm CIGSe	Mo	21.6	650	70	9.8
	300 nm SiO_2	24.8	615	68	10.3
	500 nm SiO_2	27	626	61	10.3
500 nm CIGSe	Mo	24.2	656	71	11.1
	300 nm SiO_2	27	628	72	12.2
	500 nm SiO_2	29.5	636	69	12.9

CIGSe on functional back contact with 300 nm SiO_2 scattering elements. Shunting problems were associated with thickness reduction of CIGSe solar cells, particularly when the surface roughness of the CIGSe layer is comparable to the film thickness [27]. The functional back contacts represented here have nanoelements such that their height is in the same order as the CIGSe layer thickness. Such aggressive texturing on substrates alters the growth mechanism of all the layers deposited on top as shown in the SEM image. Therefore, possible current leakage through shunt paths leads to higher shunt conductance and hence lower FF.

As a result, improved J_{sc} values by the scattering elements in combination with decreases in V_{oc} and FF lead to only a moderate increase in power conversion efficiencies. The highest efficiency of 12.9% was achieved with a 500 nm CIGSe absorber on functional back contacts with 500 nm SiO_2 scatterers, representing an absolute 1.8% increase compared to the standard solar cell design with a molybdenum back contact.

EQE curves are presented in figure 2. For the reference CIGSe solar cell on molybdenum back contact (solid black curves, figures 2(a) and (b)) the 300 nm CIGSe absorber show the lowest EQE, primarily due to incomplete absorption of the incident photons. When the CIGSe thickness increases to 500 nm (figure 2(b)), the severe absorption loss is partially resolved by a larger absorber volume. This gain in EQE starts at a wavelength of 500 nm and extends to longer wavelengths. Nevertheless, for all solar cells on a Mo back contact, the absorption loss in the near infrared region, namely at wavelengths beyond 800 nm, is large.

The simulated absorption spectra presented by black dashed lines in figure 2 for the Mo back contact are slightly higher than the measured EQE of solar cells on Mo except at wavelengths beyond 1080 nm. Moreover, calculated absorption always outperforms their experimental counterparts regardless of their back contact. The underlying reason is that recombination mechanisms, which are the source of electrical losses, were not taken into consideration in the pure optical calculations. The sharp absorption edge observed in the calculations arises due to the use of optical data that exclude any band tails or Ga grading in CIGSe. Additionally, the interference fringes in the calculated absorption spectra of the cells on Mo are slightly shifted relative to those observed experimentally. This is attributed to a slight discrepancy in the window layer thickness. Also, interface roughness, which is the natural outcome of thin film growth, is neglected by optical simulations.

The ample number of simulations we performed confirm that the absorption spectra of ultrathin CIGSe solar cells are highly sensitive to the individual layer thicknesses of the solar cell stack (not shown here). In general, for ultrathin devices, high transparency of the window layer is an essential prerequisite which is strongly dependent on the layer thicknesses. In our lab, the window layer thickness varies from batch to batch by ∼10%–15%. For dedicated samples it is possible to determine the exact thickness of the individual layers via FIB cut SEM. In figure S3, the corrected optical simulations for 500 nm CIGSe absorber with exact window layer properties extracted by UV–Vis Spectroscopy measurements and SEM imaging are shown. There is only a small difference compared to figure 2(b), underlining that these subtle differences in the theoretical absorption data cannot explain the principal discrepancies between simulation and experiment. Instead, it is the assumptions of ideal collection, neglected interface roughness, and the layer thickness variations in the optical calculations that constitute primary factors for the differences between experimental and theoretical results. Nevertheless, the solar cells on Mo back contact show a fair agreement between the simulated absorption and the experimental EQE.

Let us define $J_q = J_{sc\_exp}/J_{sc\_sim}$ to compare measured EQE and calculated absorption quantitatively, where J_{sc_exp} and J_{sc_sim} are the short circuit current densities extracted by integrating the corresponding spectra. J_q values for solar cells on Mo back contact are 96% and 93% for 300 and 500 nm CIGSe, respectively. Reaching over 93% of the calculated J_{sc} values on Mo back contact is attributed to a moderate recombination rate within the experimental solar cells, be it in the bulk or at the interfaces.

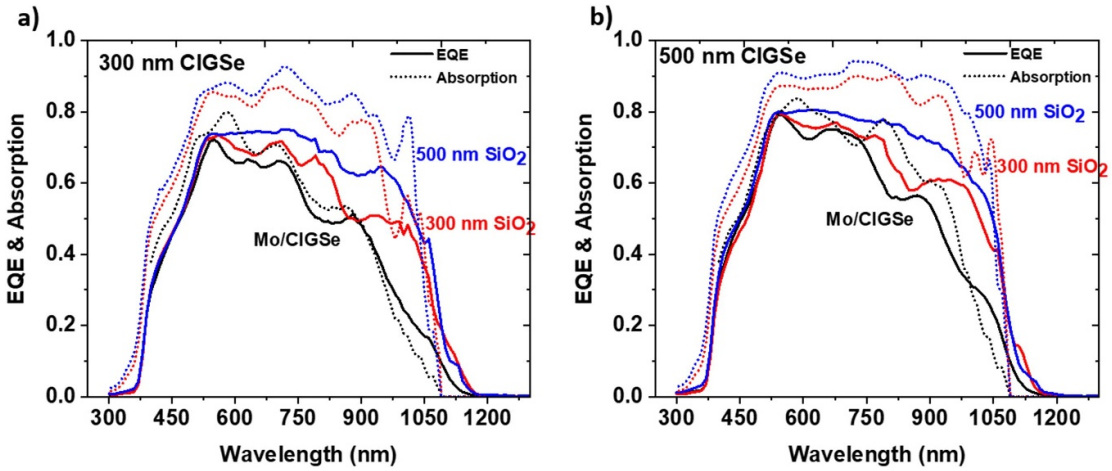

Figure 2. EQE and Absorption spectra of (a) 300 nm CIGSe, (b) 500 nm CIGSe. Solid lines are experimental EQE results while dashed lines show simulated absorption in CIGSe layer: black for Mo back contact, red and blue for 300 nm and 500 nm SiO_2 texturing element heights, respectively.

Once the functional back contacts with 300 nm SiO_2 scattering elements are implemented (solid red curves in figure 2) there is an EQE enhancement starting at 550 nm and ranging up to the absorption edge for both CIGSe thicknesses. In figure 2(a), the EQE of 300 nm CIGSe on 300 nm SiO_2 scattering elements shows interference peaks at 550, 710, 790, and 970 nm with an approximate shift of 80 nm to longer wavelengths compared to the Mo/CIGSe reference. This shift of interference peaks, together with enhanced quantum efficiency, is attributed to the effect of light management. A similar trend is observed for 500 nm CIGSe solar cells on functional back contacts with 300 nm SiO_2 scattering elements. In both cases, the enhancement of EQE is prominent in the NIR region of the spectrum. Moreover, for the 500 nm CIGSe absorber the interference oscillations at short wavelengths weaken compared to the thinner absorber. The EQE of the solar cells on nanotextured back contacts, regardless of the CIGSe thickness, shows a shift on the absorption edge to lower energies. It should be noted that the samples of each CIGSe thickness come from the same batch and thus are identical in terms of stoichiometry as shown by the GDOES profiles in figure S1. Therefore, the shift of the absorption edge is attributed to the absorption enhancement due to optical interference.

As depicted by the full blue curves in figure 2 a and b, a further increase in absorption is perceived with higher, namely 500 nm SiO_2, scattering elements. For the 300 nm CIGSe (figure 2(a)) solar cell, the EQE flattens in the short wavelength range from 500 nm to 750 nm. In figure 2(b), for 500 nm CIGSe with 500 nm SiO_2 scattering elements, the interference peaks are totally suppressed in the entire spectrum, including the long wavelength region. Here, the EE curve shows almost a rectangular shape with a well-defined plateau between 600 nm and 1000 nm. This clearly shows that the incident light is trapped in the absorber. The weakened interference fringes in EQE reveal that the resonant modes triggered by the texturing at the back provide higher absorption in CIGSe. As mentioned above, the SEM micrograph in figure 1(b) reveals that the texturing effect to a large extent translates from the structured back contact to the front layers of the solar cell. The front surface of the solar cell has periodic hills and valleys. Therefore, given the low penetration depth of high energy photons combined with the scatterers´ positions, the increase in EQE at wavelengths between 550 nm and 700 nm is interpreted as suppressed front reflection due to textured air/TCO interface. The high energy photons couple to resonant modes which are provided by a waveguide effect due to the periodic SiO_2 texturing. The suppression of front reflection is quantified using the calculated reflection and absorption spectra of the entire solar cell stacks, as presented in figure S4 for two CIGSe thickness on three different back contacts. For both CIGSe thicknesses, the reflection of solar cells on Mo back contacts remains around 15% up to a wavelength of 800 nm. This value gradually decreases as the height of the SiO_2 scattering elements increases, dropping below 5% for 500 nm CIGSe on the functional back contact. Additionally, solar cells with Mo back contacts exhibit almost no reflection around 900 nm. This is attributed to the strong parasitic absorption of the Mo back contact, where ultrathin CIGSe is transparent to lower-energy photons. This once again demonstrates that an optically superior back contact material and design are essential for achieving high-efficiency CIGSe solar cells.

The simulated spectra presented in figure 2 by dashed lines (red and blue) suggest a systematic increase in absorption as a result of light management effects by the functional back contacts following the general trend

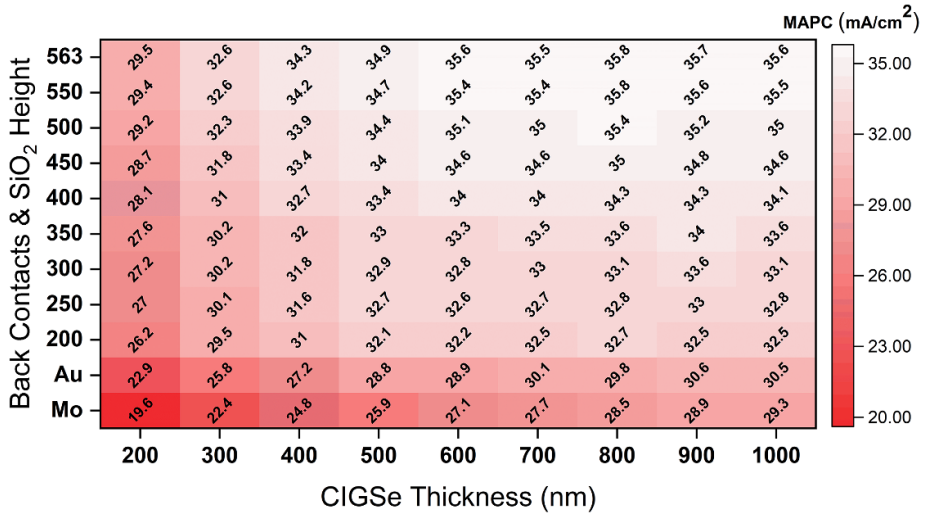

Figure 3. Heatmap scaled on maximum achievable photocurrent (MAPC) for varying CIGSe thickness and SiO_2 scattering element height.

that taller structures provide higher absorption. Thereby, a thinner CIGSe layer does not seem to allow as efficient light coupling as interference fringes are predicted by the simulation (see figures S4(b) and (c)). These two expectations from simulations are confirmed by experimental results such that higher EQE values were obtained by thicker CIGSe layers and by taller SiO_2 scattering elements. However, the J_q values principally decrease for the solar cells on functional back contacts. For the solar cells with 300 nm CIGSe and 300 nm SiO_2 height we find $J_{q\_300\_SiO2} = 82\%$ while it is $J_{q\_500\_SiO2} = 84\%$ for 500 nm SiO_2 height. The results are quite similar in the case of 500 nm CIGSe thickness, $J_{q\_300\_SiO2} = 82\%$ and $J_{q\_500\_SiO2} = 86\%$. The J_q values are noticeably smaller than in the Mo reference case.

For the short wavelength range from 420 nm to 500 nm the EQE of the structured back contacts is almost overlapping with the Mo reference. A possible reason could be incomplete collection of charge carriers due to local shunts in combination with lateral ohmic resistivity. As found in the current–voltage characteristics, there is an increased shunt conductance for the structured back contacts with 500 nm SiO_2. In order to mitigate this shunting problem and to better analyze the optical effects, the EQE and absorption curves of 500 nm CIGSe are normalized to their 550 nm wavelength values and are presented in figure S5. In this figure, the discrepancy between EQE and absorption for the solar cells on the structured back contacts is smaller but not completely removed. However, the remaining discrepancies in figure S3 can now be attributed to recombination at the different interfaces, whether at the back contact or the front contact. Due to the complex local structure of the light intensity, a simple assignment of specific recombination sites is not possible. Based on enhanced J_{sc} but reduced J_q and V_{oc} values, we conclude that the functional back contacts provide higher absorption but are prone to shunting losses as well as higher recombination.

Both simulated and experimental spectra for the two different CIGSe absorber thicknesses suggest that the EQE enhances as the height of the structuring elements increases. This finding has also been suggested by a previous work [18]. In order to confirm this tendency, further optical simulations are performed that scan a broader range of scattering element heights and CIGSe thicknesses while keeping the periodicity of the nanostructures fixed at 1 μm. Therefore, the upper limit for the SiO_2 scattering element's height, which goes up to 563 nm, is defined by the geometrical constraints of the nanotexturing. As reference current values, solar cells on standard Mo substrate and Au reflector without any scatterers are also calculated. A heat map scaled on MAPC is presented in figure 3.

Similar to the experimental results, in all simulated CIGSe thicknesses ranging from 200 nm to 1000 nm, the MAPC increases as the texturing element height increases. The highest achievable current, 35.8 mA cm^{-2}, is reached by 800 nm CIGSe on functional back contacts of 550 nm SiO_2 high. The same functional back contact results in a current density of 35.5 mA cm^{-2} with 1000 nm CIGSe absorber layer. The higher short-circuit current density achieved with a thinner absorber actually validates the influence of the light management strategy as proposed in the literature [28]. With the presence of periodic scattering elements at the back contacts, incident light waves couple into quasi-guided modes and hence provide enhanced absorption in the CIGSe layer. In this context, identifying the optimal nanotexturing parameters

should be the primary objective to achieve highly efficient ultrathin CIGSe solar cells. For instance, in [17] through optical simulations, optimum parameters were suggested as an array pitch of 550 nm, a particle radius of 250 nm and a height of 250 nm. In this work, using the specific nanotexturing geometry proposed here, we observe a continued increment in J_{sc} with scattering element height, even beyond 250 nm.

In figure 3, it is also clear that the difference between MAPC values does not change drastically over 600 nm CIGSe thickness and 450 nm SiO_2 height. MAPC for 500 nm CIGSe is only 1 mA cm^{-2} less than the maximum current value, despite 37% reduction in absorber thickness. Hence, together with experimental data and optical simulations, we conclude that the nanotexturing geometry is highly dependent on and should be considered as a coupled parameter with CIGSe thickness. Thus, by triggering the special scattering mechanisms, which is mainly accomplished by fine-tuning the light-matter interaction via geometry, the severe absorption loss of ultrathin CIGSe solar cells can be overcome.

4. Conclusion

This study demonstrates that the integration of functional back contacts with SiO_2 nano-textured scattering elements enhances the performance of ultrathin Cu(In,Ga)Se_2 solar cells. Implementation of functional back contacts leads to a notable increase in short-circuit current density, rising from 21.6 mA cm^{-2} to 27 mA cm^{-2} for a 300 nm absorber. However, this improvement comes at the cost of reduced open-circuit voltage and FF, primarily due to increased interface recombination and higher shunt conductance caused by nano-texturing. The highest efficiency of 12.9% observed for the 500 nm CIGSe absorber combined with 500 nm SiO_2 scatterers represents a 1.8% gain compared to the standard molybdenum back contact. These findings underscore the trade-offs between light management and electronic performance in ultrathin CIGSe solar cells. Both experiments and the optical simulations clearly proved that taller scattering elements are one of the key factors in order to trigger resonant modes and hence effectively compensate the absorption losses in ultrathin CIGSe solar cells. In a broader aspect, theoretical calculations reveal that by modifying the scatterer`s geometry together with the absorber thickness it is possible to have higher J_{sc} values even with thinner CIGSe layers. Overall, these findings highlight the potential of optimized nanotexturing as a viable strategy for enhancing the efficiency of ultrathin CIGSe solar cells.

Data availability statement

All data that support the findings of this study are included within the article (and any supplementary files).

Acknowledgment

This work has received funding from the European Union´s Horizon Europe research and innovation program under Grant Agreement No. 101122203 (project Hi-BITS). The authors would like to specially thank Thomas Richter for his ongoing support.

CRediT authorship contribution statement

M. Demir: Conceptualization, Data curation, Investigation, Visualization, Writing—original draft. D, Jiménez Tejero: Software, Investigation. B. Fuhrmann: Data curation, Investigation, Methodology. H. Kempa: Conceptualization, Funding Acquisition, Writing—review & editing. A. Sprafke: Conceptualization, Methodology, Software, Supervision, Writing—review & editing. R. Scheer: Conceptualization, Methodology, Funding acquisition, Supervision, Writing—review & editing.

References

[1] Gloeckler M and Sites J R 2005 Potential of submicrometer thickness Cu (In, Ga) Se 2 solar cells *J. Appl. Phys.* **98** 103703
[2] Scheer R and Schock H-W 2011 *Chalcogenide Photovoltaics: Physics, Technologies, and Thin Film Devices* (Wiley) (available at: https://cds.cern.ch/record/1613202)
[3] Mansfield L M, Kanevce A, Harvey S P, Bowers K, Beall C, Glynn S and Repins I L 2018 Efficiency increased to 15.2% for ultra-thin Cu(In,Ga)Se_2 solar cells *Prog. Photovolt., Res. Appl.* **26** 949–54
[4] Oliveira A *et al* 2023 Over 100 mV V_{OC} improvement for rear passivated ACIGS ultra-thin solar cells *Adv. Funct. Mater.* **33** 2303188
[5] Green M A, Dunlop E D, Yoshita M, Kopidakis N, Bothe K, Siefer G, Hinken D, Rauer M, Hohl-Ebinger J and Hao X 2024 Solar cell efficiency tables (Version 64) *Prog. Photovolt., Res. Appl.* **32** 425–41
[6] Krc J, Sever M, Campa A, Lokar Z, Lipovsek B and Topic M 2017 Optical confinement in chalcopyrite based solar cells *Thin Solid Films* **633** 193–201

[7] Kovacic M et al 2019 Light management design in ultra-thin chalcopyrite photovoltaic devices by employing optical modelling *Sol. Energy Mater. Sol. Cells* **200** 109933
[8] Ji C, Liu W, Bao Y, Chen X, Yang G, Wei B, Yang F and Wang X 2022 Recent applications of antireflection coatings in solar cells *Photonics* **9** 906
[9] Yin G, Knight M W, van Lare M-C, Solà Garcia M M, Polman A and Schmid M 2017 Optoelectronic enhancement of ultrathin $CuIn_{1-x}Ga_xSe_2$ solar cells by nanophotonic contacts *Adv. Opt. Mater.* **5** 1600637
[10] Shin M J et al 2021 Semitransparent and bifacial ultrathin Cu (In, Ga) Se_2 solar cells via a single-stage process and light-management strategy *Nano Energy* **82** 105729
[11] Li Y, Tabernig S W, Yin G, Polman A and Schmid M 2022 Beyond light-trapping benefits: the effect of SiO2 nanoparticles in bifacial semitransparent ultrathin Cu (In, Ga) Se_2 solar cells *Sol. RRL* **6** 2200695
[12] Wang W, Zhang J, Che X and Qin G 2016 Large absorption enhancement in ultrathin solar cells patterned by metallic nanocavity arrays *Sci. Rep.* **6** 34219
[13] Schmid M 2017 Review on light management by nanostructures in chalcopyrite solar cells *Semicond. Sci. Technol.* **32** 43003
[14] Jarzembowski E, Fuhrmann B, Leipner H, Fränzel W and Scheer R 2017 Ultrathin Cu (In, Ga) Se_2 solar cells with point-like back contact in experiment and simulation *Thin Solid Films* **633** 61–65
[15] Chen S-C et al 2014 Toward omnidirectional light absorption by plasmonic effect for high-efficiency flexible nonvacuum Cu (In, Ga) Se_2 thin film solar cells *ACS Nano* **8** 9341–8
[16] Massiot I, Cattoni A and Collin S 2020 Progress and prospects for ultrathin solar cells *Nat. Energy* **5** 959–72
[17] Van Lare C, Yin G, Polman A and Schmid M 2015 Light coupling and trapping in ultrathin Cu (In, Ga) Se_2 solar cells using dielectric scattering patterns *ACS Nano* **9** 9603–13
[18] Schneider T, Tröndle J, Fuhrmann B, Syrowatka F, Sprafke A and Scheer R 2020 Ultrathin CIGSe solar cells with integrated structured back reflector *Sol. RRL* **4** 2000295
[19] Demir M, Sprafke A, Fuhrmann B, Schneider T, Hölscher T, Kempa H and Scheer R 2023 Photon management by functional back contacts for ultrathin cigse solar cells: insights from experiment and simulation *40th European Photovoltaic Solar Energy Conf. and Exhibition (EU PVSEC)* (https://doi.org/10.4229/EUPVSEC2023/2DO.6.4)
[20] Facchini A 2018 Laser interference lithography technique for back-contact microstructuring of CuIn $(1-x)$ $GaxSe_2$ solar cells *MS Thesis* Luther University Halle-Wittenberg, Germany pp 1–71
[21] Gabor A M, Tuttle J R, Bode M H, Franz A, Tennant A L, Contreras M A, Noufi R, Jensen D G and Hermann A M 1996 Band-gap engineering in Cu (In, Ga) Se_2 thin films grown from (In, Ga) $2Se_3$ precursors *Sol. Energy Mater. Sol. Cells* **41–42** 247–60
[22] Pomplun J, Burger S, Zschiedrich L and Schmidt F 2007 Adaptive finite element method for simulation of optical nano structures *Phys. Status Solidi b* **244** 3419–34
[23] Querry M R 1987 *Optical Constants of Minerals and Other Materials from the Millimeter to the Ultraviolet Tech. Rep. CRDEC-CR-88009* ADA192210 (Defense Technical Information Center (DTIC))
[24] McPeak K M, Jayanti S V, Kress S J P, Meyer S, Iotti S, Rossinelli A and Norris D J 2015 Plasmonic films can easily be better: rules and recipes *ACS Photonics* **2** 326–33
[25] Orgassa K 2004 Coherent Optical Analysis of the ZnO/CdS/Cu (In, Ga) Se_2 Thin Film Solar Cell (Shaker)
[26] Naghavi N et al 2017 Ultrathin Cu (In, Ga) Se_2 based solar cells *Thin Solid Films* **633** 55–60
[27] Lundberg O, Bodegård M, Malmström J and Stolt L 2003 Influence of the Cu (In, Ga) Se_2 thickness and Ga grading on solar cell performance *Prog. Photovolt., Res. Appl.* **11** 77–88
[28] Dahan N et al 2012 Optical approaches to improve the photocurrent generation in Cu (In, Ga) Se_2 solar cells with absorber thicknesses down to 0.5 μm *J. Appl. Phys.* **112** 94902